Observation of Two-source Interference in the Photoproduction Reaction $AuAu \to AuAu\rho^0$

The STAR collaboration

Abstract

In ultra-peripheral heavy ion collisions, a photon from the electromagnetic field of one nucleus can fluctuate to a quark-antiquark pair and scatter from the other nucleus, emerging as a ρ^0. The ρ^0 production is well localized at the two nuclei, forming a 2-source interferometer. At low transverse momenta, the ρ^0 amplitudes from the two sources interfere destructively, suppressing production. We measure this interference in 200 GeV per nucleon Au-Au collisions, and observe interference at $96 \pm 5 \pm x\%$ of the expected level, and find a maximum decoherence, due to wave function collapse or other factors, of x% at the 90% confidence level.

Electromagnetic interactions between relativistic heavy ions are relatively simple. The ions act as sources of quasi-real virtual photons, and their internal structure is unimportant. A variety of two-photon and photonuclear interactions have been discussed[1]. In coherent vector meson production, a photon from the field of one nucleus fluctuates into a quark-antiquark pair which scatters elastically from the other nucleus, emerging as a vector meson. This reaction has a large cross section, about 8-10% of the hadronic cross section for gold-gold collisions at a center of mass energy of 200 GeV per nucleon[2][3][4].

We have observed interference between ρ^0 production by the two ions in gold-gold UPCs. The interference is $96 \pm 5 \pm xx\%$ of the maximal interference. The space-time development of the $\pi\pi$ final state requires that this interference involved well-separated pion pairs. This is an example of the Einstein-Podolsky-Rosen paradox, and demonstrates that the ρ^0 decay does not collapse the wave function.

The ρ^0 production can occur at impact parameters b much larger than twice the nuclear radii R_A. Because the $(q\overline{q})N$ scattering involves the short-ranged strong force, the ρ^0 production occurs in or very near (within 1 fm) the two ions, so the system consists of two well-separated sources. There are two possibilities: either nucleus 1 emits a photon which scatters off nucleus 2, or vice versa. These two possibilities are indistinguishable here, so the amplitudes add; because vector mesons are negative parity, the amplitudes actually subtract with a transverse momentum (p_T) dependent phase factor to account for the separation. The cross section is [5]

$$\sigma = |A_1 - A_2 \exp{(i\vec{p_T} \cdot \vec{b})}|^2 \tag{1}$$

where A_1 and A_2 are the amplitudes for ρ^0 production from the two directions of b. For the ρ^0, the cross-section rises only slowly with energy, so δ, the production phase difference, should be negligible. At mid-rapidity $A_1 = A_2$ and

$$\sigma = \sigma_0[(1 - \cos{(p_T \cdot b)}] \tag{2}$$

where σ_0 is the cross section without interference. The system acts as a 2-slit interferometer, with slit separation b. As b is unmeasured, the observed p_T spectrum is obtained by integrating Eq. (1) over b. The p_T spectrum is suppressed for $p_T <\sim \hbar/|!\langle b\rangle$. where $\langle b\rangle$ is the mean impact parameter.

There are at least two theoretical calculations of this inteference. Klein and Nystrand (KN) [5] calculate the interference with a detailed form factor in a model where the inter-

ference was calculated from the centers of the two nuclei. Hencken, Baur and Trautmann (BHT)used a more detailed model of the photon profile and a simple Gaussian form factor for the nucleus [6]; unfortunately, the HBT calculation only considered production at mid-rapidity (y=0), and so cannot be directly compared with data. At $y = 0$, the two calculations agree fairly well.

In this letter we measure this interference in 200 GeV per nucleon gold on gold collisions by studying the transverse momentum (p_T) spectrum of photoproduced ρ^0. We also set limits on possible decoherence due to external factors. This data was taken with the STAR detector. The major components used in this analysis are the central time projection chamber (TPC) [7], a solenioidal magnet with a 0.5 T field, and two trigger detectors. The TPC was sensitive to charged particles with psuedorapidity $|\eta| < 1.0$. The central trigger barrel (CTB) consisted of 240 scintillator slats surrounding the TPC, detecting charged particles with pseudorapidity $|\eta| < 1.0$ [8]. The zero degree calorimeters (ZDCs) detected neutrons released at low p_T when the gold nuclei dissociated [9].

Data was taken with two separate triggers. One trigger selected events compatible with ρ^0 photoproduction accompanied by mutual Coulomb excitation, while the other selected ρ^0 events irrespective of nuclear excitation. Photoproduction accompanied by mutual Coulomb excitation proceeds largely by three-photon exchange - one photon for the ρ^0, and one to excite each nucleus. The individual sub-reactions are independent, and at a given impact parameter b, the cross-section for $n-$photon reactions factorizes, and the probability for an n photon reaction is $P_n(b) = \prod_{i=1}^{n} P_i(b)$ [10]. The shared b leads to very different impact-parameter distributions for the two processes which in turn alters the ρ^0 p_T spectrum[11].

The topology trigger selected exclusive ρ^0 events with roughly back-to-back pions in the CTB [3]. About 1.5 million triggers were used in this analysis. The minimum bias trigger selected events where both nuclei dissociated, and released neutrons into the two ZDCs.

Data from both triggers was processed identically, except that events from the CTB based trigger were distributed more broadly along the TPC axis, and consequently, were accepted in a wider region. For the topology data, we exclude events with a ρ^0 rapidity $|y| < 0.05$ to avoid any possible contamination from cosmic rays,where a single track could be reconstructed as a pair with net charge 0, $p_T = 0$ and $y = 0$.

The event selection produced a clean set of ρ^0 events, at some cost in efficiency. Events were required to have net charge zero and exactly two tracks with a vertex within 50 cm

longitudinally of the center of the TPC for the minimum bias sample, and 100 cm for the topology sample. The tracks were assumed to be pions, and were required to have a $\pi\pi$ invariant mass 550 MeV $< M_{\pi\pi} <$ 920 MeV.

The background was estimated by looking at like-sign pion pairs, and was found to be small, 1.4%. Figure **??** compares the rapidity and $M_{\pi\pi}$ distributions of the data and our simulations.

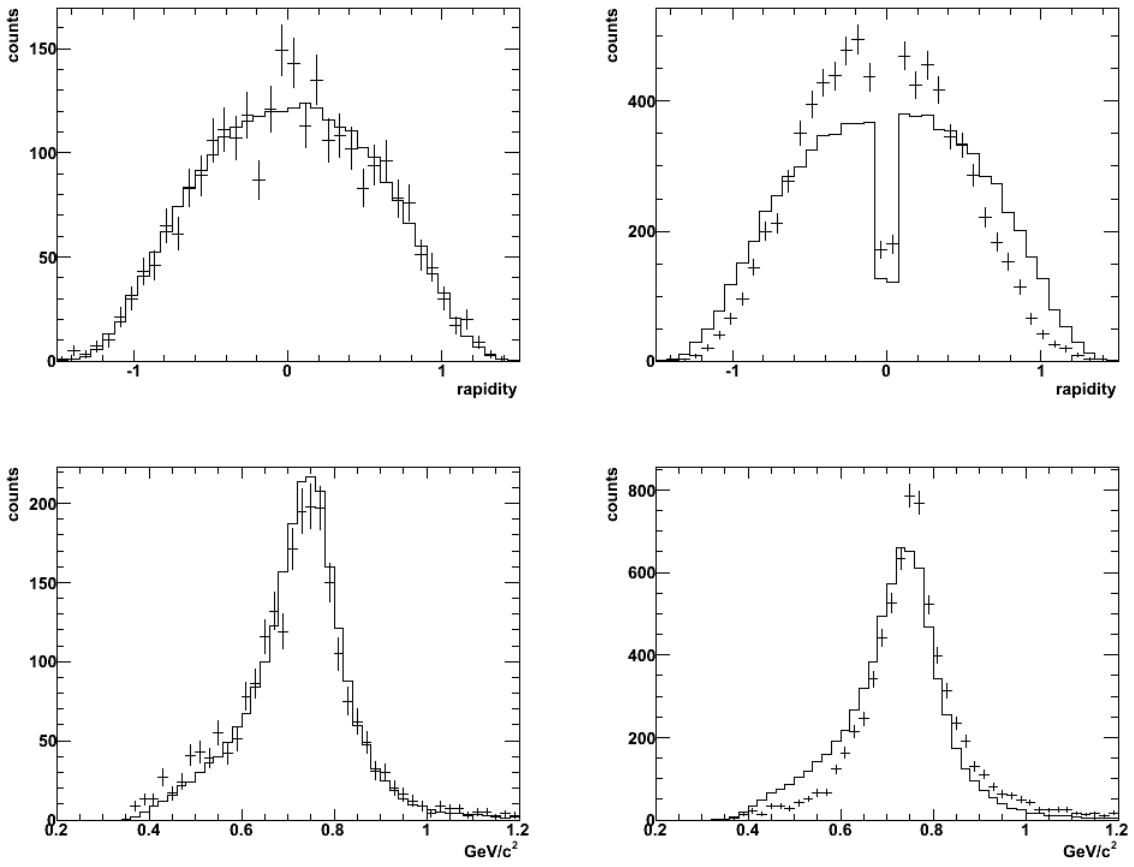

FIG. 1: The rapidity (top) and $M_{\pi\pi}$ (bottom) distributions for the topology (exclusive ρ^0) sample (right) and minimum bias (Coulomb breakup) sample (left). The points with error bars are the data, and the histograms are the simulations.

These data includes directly produced $\pi^+\pi^-$ pairs [12] along with the ρ^0. These channels are indistinguishable, so the two processes interfere. The direct pion rate is relatively small, but interference between $\rho^0 \rightarrow pi^+\pi^-$ and directly produced $\pi^+\pi^-$ shifts the observed ρ^0 mass peak to a lower mass value. The observed shift and direct pion fraction are consistent

with earlier AuAu photoproduction [3] and fixed target photoproduction experiments[13] The direct pions should have the same spin/parity and quantum mechanical behavior as the $\pi^+\pi^-$ from ρ^0 decay, so we do not distinguish between the two sources. With the chosen mass cut, background from misidentified two-photon production of lepton pairs should be very small.

The interference depends on the amplitudes for ρ^0 production by the two nuclei, which themselves depend on the photon energies., Away from $y = 0$, the photon energies differ, $k_{1,2} = M_V/2 \exp(\pm y)$, so the amplitudes differ and the interference is less than maximal. Although it is not expected in the soft-Pomeron model, the the photon energy difference could introduce a small ρ^0 production phase difference, which could affect the interference[14]. This paper focuses on the region near mid-rapidity where we assume that this phase difference is small.

To study the interference, we use the variable $t_\perp = p_T^2$. At RHIC energies, the longitudinal component of the 4-momentum transfer is small, so $t \approx t_\perp$. $t_\perp$ is convenient because, without interference, the spectrum dN/dt is well described by an exponential distribution for a wide variety of nuclear models. KN use a Woods-Saxon distribution for the gold density distribution, while BHT use a Gaussian distribution; both are quite well fit by an exponential distribution[19][5]. To determine the interference in different rapidity bins, we use a Monte Carlo simulation which follows Refs. [2] and [5].

Figure 2 compares the uncorrected minimum bias data for $|\eta| < 0.5$ with simulation with interference ("Int") and without it ("Noint"). The dN/dt spectrum shows a significant downturn for $t < 0.015$ GeV^2. This drop is consistent with the simulation.

The efficiency corrected data are shown in Fig. 3. Minimum bias and topology data are shown separately, each with three rapidity bins: $0.05 < |y| < 0.5$ topology, $0.0 < |y| < 0.5$ minbias, and $0.5 < |y| < 1.0$ for both. The efficiency is independent of p_T, but p_T smearing (resolution) in the affects the spectrum slightly. The ρ^0 p_T resolution is about 9 MeV/c, compared to the first t bin width of (15 MeV/c)^2. Momentum resolution depletes the first few bins, but feeddown from the higher t bins partially repopulates them. We will discuss the accuracy of the data correction later.

The dN/dt spectrum is fit by the 3-parameter form:

$$\frac{dN}{dt} = A \exp(-kt)[1 + c(R(t) - 1)] \tag{3}$$

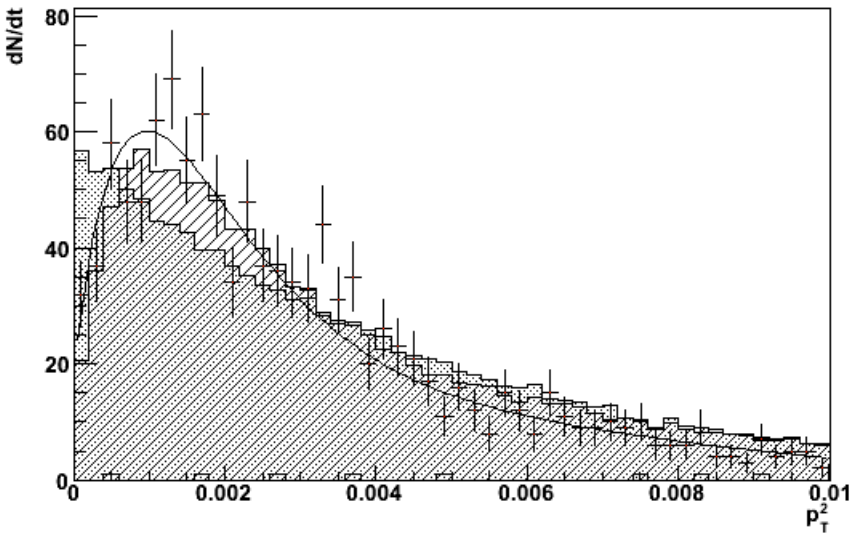

FIG. 2: Raw (uncorrected) $t_\perp$ spectrum for ρ^0 sample for $0.0 < |y| < 0.5$ for the minbias data. The points are the data, while the diagonally hatched histogram is a simulation assuming that there is interference; the overlapping filled histogram is a simulation without interference. The dashed histogram is the wrong-sign background.

where

$$R(t) = \frac{Int(t)}{Noint(t)} \tag{4}$$

is the ratio of the t-spectra with and without interference. Here, A is the overall normalization necessary to the fit but without significance to the measurement, the slope k is related to the nuclear radius, c gives the degree of spectral modification; $c = 0$ corresponds to no interference while $c = 1$ is the expected interference.

$R(t)$ was calculated using a Monte Carlo simulation with the correct ρ^0 rapidity dependence. For $t > 0.1GeV^2$, the interference and no-interference calculations coincide, and $R(t) \to 1$. In the t region considered here, $R(t) \neq 1$; no normalization is applied.

The Monte Carlo $R(t)$ were fit by an analytic function. We use several different functions to fit $R(t)$ to Monte Carlo simulations. Since $R(t)$ varies most rapidly at small t, we fit it to a polynomial of the form $R(t) = \Sigma_{i=0}^{n} a_i/(t + 0.012\mathrm{GeV}^2)^i$, where 0.012 GeV^2 has no physical significance and could be varied considerably with little effect.

Table 1 gives the results of the standard fit. In the small-rapidity samples, where A_1 and A_2 are similar, the interference is much larger. It is also much larger in the minbias data

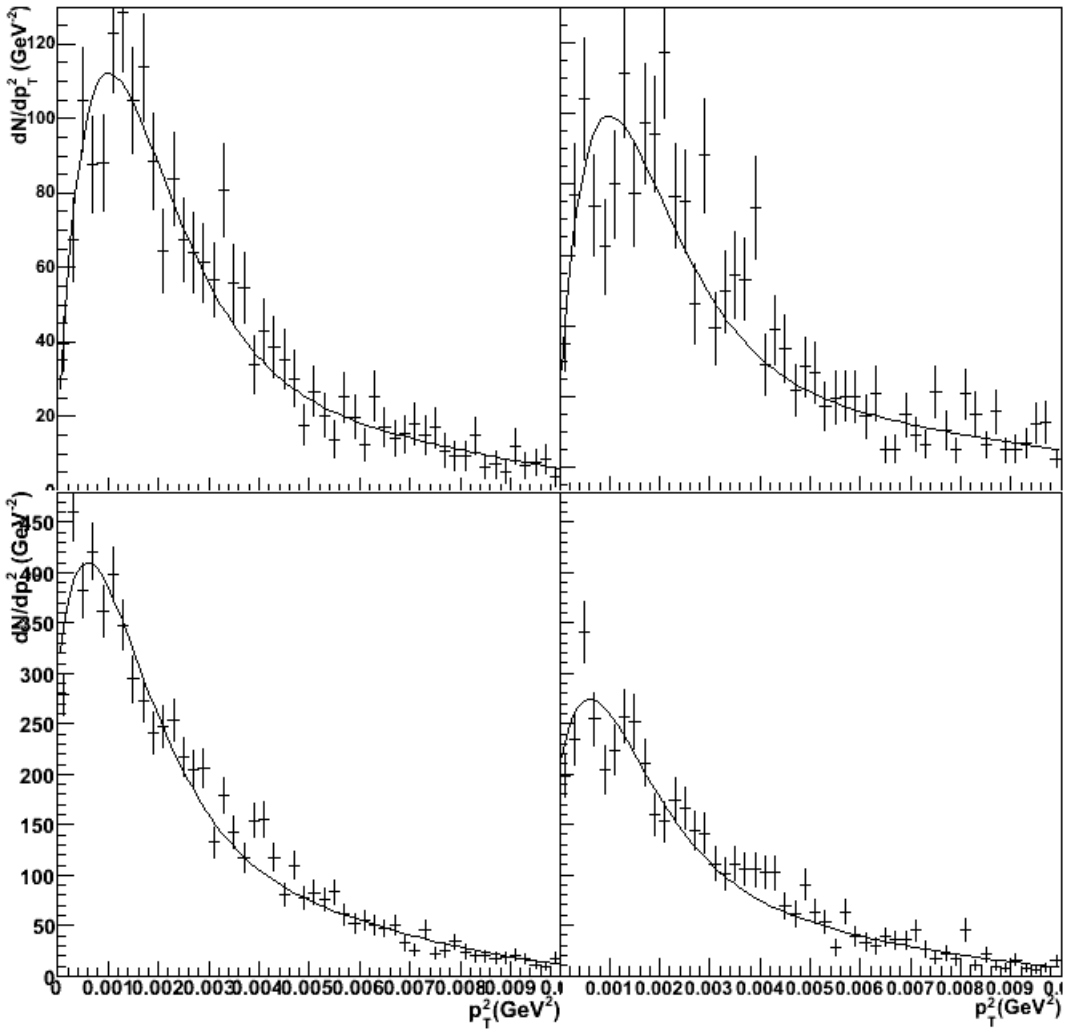

FIG. 3: Efficiency corrected $t_\perp$ spectrum for ρ^0 from (a) mutual dissociation with $0.0 < |y| < 0.5$, (b) mutual dissociation with $0.5 < |y| < 1.0$, (c) topology trigger with $0.05 < |y| < 0.5$ and (d) topology trigger with $0.5 < |y| < 1.0$. The histograms are the data, while the solid line is a simulation assuming that there is interference; the dashed line is a simulation without interference. The dashed histogram is the like-sign background.

than the topology data. This is because the median impact parameter in the minimum bias data is theoretically much smaller than in the topology data.

The 4 c values are consistent within errors; the weighted average is $c = 0.96 \pm 0.05$. The k values for the minimum bias and exclusive ρ^0 data differ by xx%: $xxx \pm x$ GeV^{-2} for the exclusive ρ^0 versus $xxx \pm xx$ GeV^{-2} for the Coulomb breakup events.

The different k values may be attributed to the different impact parameter distributions.

Trigger	Rapidity	A	b	c	Background (%)	χ^2/DOF
MinBias	$\|y\| < 0.5$	6493 ± 304	299 ± 12	0.92 ± 0.07	0.68%	43/47
MinBias	$0.5 < \|y\| < 1.0$	5646 ± 334	304 ± 15	0.93 ± 0.09	0.94%	75/47
Topo	$0.1 < \|y\| < 0.5$	8870 ± 210	356 ± 7.0	0.91 ± 0.11	1.4%	80/47
Topo	$0.5 < \|y\| < 1.0$	9815 ± 333	351 ± 9.0	0.98 ± 0.20	1.7%	88/47

TABLE I: Fits to the 4 data sets. The χ^2/DOF are discussed in the systematic errors.

The photon flux at an impact parameter b scales as $1/b^2$. When b is only a few times R_A, ρ^0 are more likely to be produced on the side of the target near the photon emitter. The resulting peak in the ρ^0 production amplitude leads to a smaller effective production volume and the smaller b. This near-side skewing also affects the interference slightly. This effect is not considered in our simulations, and is discussed under systematic errors.

We have studied four classes of systematic errors in this measurement: instrumental, background, fitting, and theoretical. The instrumental studies looked at a number of variables. The vertex position, rapidity distribution, $M_{\pi\pi}$ distribution, and $\pi^{\pm}$ angular distributions agree well between the data and simulation. This analysis is most sensitive to any ρ^0 p_T-dependent variation in the efficiency, or p_T smearing. The ρ^0 p_T resolution is about x MeV/c; this leads to significant smearing only in the two lowest $t_\perp$ bins. As a test of the sensitivity of the fit to the p_T resolution, we fit the raw (uncorrected) t spectrum with the raw Monte Carlo output; this reduced c by 0.xx, mostly due to smearing in the lowest t bins. Based on these tests, we assign a 4% systematic errors to c due to detector effects.

Backgrounds are a small effect. Backgrounds were estimated using like-sign pairs ($\pi^+\pi^+ + \pi^-\pi^-$). The like-sign background percentages with $t < 0.01$ GeV^2 region are given in Table 1. They are $\approx 2\%$ of the spectrum. The like-sign backgrounds should be within a factor of 2 of the true background [3]; this leads to an x% systematic error due to the backgrounds.

The uncertainty due to fitting was evaluated by comparing fits with different $R(t)$: 5th and 6th order 'inverted' polynomials and 5th and 6th order polynomials. c varied by an average of y%; we use this as the systematic error. There could also be some error introduced if the spectrum without interference is not a perfect exponential in t. We also studied the correlations between 'b' and 'c'. When b is changed by x% in the input simulation, c changed

Source	Uncertainty (%)
Detector Corrections	x
Backgrounds	x
Fitting	x
Theoretical Model	x
Nuclear radius skewing	x
Total	x

TABLE II: Systematic Errors and their size.

by y%. Overall, we assign an x% systematic error due to the fitting procedure.

The sytematic error due to theoretical uncertainties is the largest error. The KN and BHT models are in reasonably good agreement with each other. However, the poor χ^2/DOF for the minimum bias $0.5 < |y| < 1.0$ and topology $0.05 < |y| < 0.5$ datasets may point to a problem with the theoretical input curves. These poor χ^2 are generally stable with respect to variations in data selection criteria, fit functions, and reasonable variations in the nuclear radii in the simulations.

To account for the bad χ^2/DOF, we followed the particle data group procedure [18] and scaled up the statistical errors in the fits by $\sqrt{\chi^2/DOF}$. We quadrature subtract the unscaled statistical error, and attribute the remaining error to systematic error due to the model. Since there is no reason to expect the theory to be better or worse for the four datasets, we average the four systematic errors and assign that to all four fits. We also add a 5% systematic error in quadrature to account for the skewing in the nuclear radii - in effect the correlation between k and c in the fits.

With these errors, we combine the four reasults, and find that interference is $xx \pm xx \pm xx\%$ of that expected. Thus, the decoherence $\xi = 1 - c$ due to wave function collapse or environmental factors is is less than 40% at the 90% confidence level.

Because the ρ^0 decay so rapidly, $\gamma\beta c\tau \ll \langle b \rangle$, the ρ^0 decay points are well separated in space-time, so the ρ^0 decays occur before the wave functions from the two production points overlap. Any interference must involve the $\pi\pi$ final states[15]. For this interference to be possible, the post-decay $\pi\pi$ wave functions must retain components for all possible ρ^0

decays, and must not collapse before the wave functions from the two ion sources overlap. This requires a non-factorizable (non-local) wave function and is thus an example of the Einstein-Podolsky-Rosen paradox [16].

[1] C. A. Bertulani, S. R. Klein and J. Nystrand, Ann. Rev. Nucl. Part. Sci. **55**, 271 (2005); G. Baur *et al.*, Phys. Rep. **364**, 359 (2002); F. Krauss, M. Greiner and G. Soff, Prog. Part. Nucl. Phys. **39**, 503 (1997).

[2] S. Klein and J. Nystrand, Phys. Rev. **C60**, 014903 (1999).

[3] C. Adler *et al.*, Phys. Rev. Lett. **89**, 027302 (2002).

[4] L. Frankfurt, M. Strikman and M. Zhalov, Phys. Rev. **C67**, 034901 (2003); L. Frankfurt, M. Strikman and M. Zhalov, Phys. Lett. **B537**, 51 (2002).

[5] S. Klein and J. Nystrand, Phys. Rev. Lett. **84**, 2330 (2000).

[6] K. Hencken, G. Baur and D. Trautmann, Phys. Rev. Lett. **96**, 012303 (2006).

[7] M. Anderson *et al.*, Nucl. Instrum & Meth. **B499**, 659 (2003); M. Anderson *et al.*, Nucl. Instrum & Meth. **B499**, 679 (2003).

[8] F. S. Bieser *et al.*, Nucl. Instrum & Meth. **B499**, 766 (2003).

[9] C. Adler *et al.*, Nucl. Instrum. & Meth. **A470**, 488 (2001).

[10] G. Baur *et al.*, Nucl. Phys. **A729**, 787 (2003).

[11] A. Baltz, S. Klein and J. Nystrand, Phys. Rev. Lett. **89**, 012301 (2002).

[12] P. Söding, Phys. Lett. **B19**, 702 (1966).

[13] Fixed target photoproduction.

[14] T. H. Baur *et al.*, Rev. Mod. Phys. **50**, 261 (1978).

[15] S. Klein and J. Nystrand, Phys. Lett. **A308**, 323 (2003).

[16] A. Einstein, B. Podolsky and N. Rosen, Phys. Rev. **47**, 777 (1935).

[17] M. Vidovic, M. Greiner, C. Best and G. Soff, Phys. Rev. **C47**, 2308 (1993); G. Baur and L. G. Ferreira Filho, Phys. Lett. **B254**, 30 (1991).

[18] W.-M. Yao *et al.*, J. Phys. G**33**, 1 (2006).

[19] G. McClellan *et al.*, Phys. Rev. **D4**, 2683 (1971).